Lumped Reaction Kinetic Models for Pyrolysis of Heavy Oil in the Presence of Supercritical Water

Qing-Kun Liu, Dao-Qi Zhu, Xue-Cai Tan, Pei-Qing Yuan, Zhen-Min Cheng, and Wei-Kang Yuan
State Key Laboratory of Chemical Engineering, East China University of Science and Technology, Shanghai 200237, China

Jing-Yi Yang
Research Institute of Petroleum Processing, East China University of Science and Technology,
Shanghai 200237, China

DOI 10.1002/aic.14978

The reaction kinetics of the pyrolysis of heavy oil in the presence of supercritical water (SCW) and high pressure N_2 were measured. At any reaction temperature applied, the pyrolysis under SCW environments is faster than that under N_2 environments. Meanwhile, at lower temperatures the pyrolysis under both environments is accelerated by the introduction of coke into the feedstock. On the basis of a first-order four-lump reaction network consisting of the sequential condensation of maltenes and asphaltenes, the pyrolysis in whichever medium can be preferably described either by the lumped reaction kinetic model modified with autocatalysis and pseudoequilibrium or by the model modified solely with pseudoequilibrium. Benefited from the reduced limitation of diffusion to reaction kinetics, the pyrolysis in the SCW phase is more sensitive to the increase in reaction temperature than that in the oil phase, disengaging readily from the dependence on autocatalysis at a lower temperature. © 2015 American Institute of Chemical Engineers *AIChE J*, 62: 207–216, 2016
Keywords: lumped reaction kinetic model, pyrolysis, heavy oil, supercritical water, autocatalysis

Introduction

Some of the largest reserves in the world are heavy oil reservoirs with oil in place equaling to the conventional oil fields in the Middle East. The exploitation of heavy oil becomes mature with the aid of steam assisted gravity drainage, *in situ* combustion and other techniques.[1–3] Nowadays, refineries worldwide are facing challenges to process unconventional heavy oil containing high contents of carbon residue and heteroatoms. Among the technologies available, pyrolysis, which follows the mechanism of “carbon rejection,” is always an alternative solution for processing inferior heavy oil.[4,5]

Since the 1990s, the pyrolysis, hydrocracking and extraction of heavy oil in the presence of supercritical water (SCW, T_c=647 K, P_c=22.1 MPa) have received increasing attention in academia.[6–13] It was believed that the upgrading, desulfurization, denitrification, and demetalization of heavy oil could be accomplished simultaneously by the special properties of SCW; that is, a nonpolar solvent with excellent solubility and diffusivity, an effective acid/base catalyst and even a H-donor. A considerable number of related studies have been reported from different aspects. Erkey and coworker and Timko et al. presented comprehensive reviews on recent findings in this field.[14,15] Based on theoretical calculation, Kida et al. deduced that alkyl sulfides contained in heavy oil may decompose in SCW with a free radical mechanism during which SCW acts as a reactant and a catalyst.[16] However, heterocyclic compounds were reported to be rather stable in SCW.[17,18] By introducing the partial oxidation of hydrocarbons in SCW, Adschiri et al. and Yuan et al. found that heterocyclic compounds were partly removed through the *in situ* water-gas shift and the subsequent hydrogenation on sulfided NiMo and CoMo catalysts in series.[19–21] Many a research now considered SCW as an inert reaction medium for the pyrolysis of heavy oil, a process participated mainly by carbon radicals on polycyclic aromatics and substitutes.[13,22] According to the degradation of polyethylene in SCW using D_2O as a tracer, SCW can only participate in the pyrolysis of hydrocarbons through the hydration with alkene products in the ionic mechanism.[23,24] The quantum mechanism based calculation also denies the possibility of the direct H-abstraction of carbon radicals from water.[25]

Despite of some common understandings achieved, there, however, exist a serious disagreement over the essential issues of the pyrolysis of heavy oil in SCW; that is, whether the yield of light oil fractions could be increased and the formation of coke could be suppressed.[13,22,26–28] The contradictory conclusions reported in the literature were caused largely by the fact that the knowledge about the phase structure and the reaction kinetics of the upgrading of heavy oil in the presence of SCW is far from sufficient.

According to the definition of van Konynenburg and Scott, the mixture of heavy oil and water follows the type IIIb phase

---

Correspondence concerning this article should be addressed to P.-Q. Yuan at pqyuan@ecust.edu.cn.

Table 1. Properties of the Raw Heavy Oil

Molecular Weight (kg/kmol)	API Gravity (°)	Dynamic Viscosity (353 K, Pa s$\times 10^3$)	H/C Ratio	Maltenes (wt %)	Asphaltenes (wt %)
811	14	2931.58	1.41	95.0	5.0

behavior.[29,30] The LLV three-phase equilibrium curve of the mixture extends from low temperature up to the vicinity of the critical point of water, intersected by the liquid-vapor critical locus extending from the critical point of water. Above the upper critical point temperature of the LLV curve, the water-rich liquid phase and the vapor phase become identical. With the oil/water two-phase structure, the nonpolar fraction of maltenes is extracted substantially into the SCW phase, leaving asphaltenes highly concentrated in the oil phase.[28] Meanwhile, a limited amount of water is solubilized into the oil phase.[31] Once the pyrolysis network is initiated at a high enough temperature, the reaction occurs simultaneously in the oil and SCW phases.

As the pyrolysis proceeds, polycyclic aromatics in the boiling point ranges of diesel and gasoline are produced. The mixture of polycyclic aromatics and water follows the type II phase behavior in which the critical points of water and hydrocarbons are connected by a vapor-liquid critical line.[32] Under the commonly adopted upgrading conditions, that is, temperatures higher than 663 K and pressures higher than 22.1 MPa, the mixture of liquid pyrolysis products and SCW should exist in the single phase structure. At that time, the pyrolysis occurs exclusively in the SCW phase. One may reasonably deduce that a transition from the oil/water two-phase structure to the single-phase structure can be observed sooner or later during the pyrolysis of heavy oil in SCW. Such a deduction was confirmed by Vilcaez et al. who observed the disappearance of the phase boundary between the oil and water phases in the upgrading of bitumen in SCW at the mass ratio of water to oil of 2.5:1 and the temperature of 713 K.[33]

The introduction of SCW into the upgrading of heavy oil makes it possible that the pyrolysis occurs not only in the oil phase but also in the SCW phase. The resulted differences in fraction distribution and diffusion thus may exert influence on the reaction kinetics of those free radical reactions involved. An analysis from the reaction kinetic point of view should be helpful to an in-depth understanding of the upgrading of heavy oil in the presence of SCW. There is no doubt that an appropriate reaction kinetic model is the prerequisite for the investigation on reaction kinetics. Unfortunately, the reaction kinetic models available, mostly based on lumping approaches, were developed according to the pyrolysis under N_2 environments without exception. Whether these lumped models can be applied to the pyrolysis under SCW environments has not been strictly verified so far.

On the basis of the preceding study on the pyrolysis of heavy oil in the presence of dense SCW and high pressure N_2, the corresponding kinetic data were re-examined and supplemented further.[34] Also, the autocatalytic characteristic of pyrolysis was experimentally examined. With a four-lump reaction network, the traditional first-order reaction kinetic model was modified with different hypotheses. The kinetic parameters of the models suggested were then estimated, followed by an evaluation on their adaptability to the pyrolysis occurring in the SCW and oil phases. Finally, the effect of reaction media on the reaction kinetics of the pyrolysis of heavy oil was discussed.

Experimental

A Parr 4598-HPHT autoclave with a capacity of 0.1 L was used in the pyrolysis of heavy oil under SCW and N_2 environments. The raw heavy oil whose properties are listed in Table 1 was obtained from Sinopec Shanghai Petrochemical Company. According to thermogravimetric analysis, the heavy oil starts cracking at the temperature around 623 K but the maximum rate of weight loss occurs at the temperature of 720 K.

For the pyrolysis under SCW environments, the reactor was charged with heavy oil of 10 g and water of 25 g. For the pyrolysis under N_2 environments, the reactor was charged with 20 g of heavy oil and N_2 of 8.0–9.0 MPa. The sealed reactor was heated from the ambient temperature to the reaction temperature at a slope of 15 K/min, during which the stirring rate was kept at 200 rpm. Once the reaction temperature reached a preset value between 663 and 703 K, the stirring rate was adjusted to 800 rpm immediately. Finally, the reaction lasting 15 min to 12 h was terminated by subjecting the reactor in forced air cooling. To examine the autocatalytic characteristic of pyrolysis, coke, which was collected in pyrolysis and grinded to a size distribution between 50 and 75 μm, was added as the catalyst into the feedstock. The mass ratio of coke to heavy oil varied from 1:100 to 1:20. Other operating procedures were just the same with the pyrolysis without the addition of coke. To ensure that the maximum error of product distribution falls within a reasonable range of ±5%, all the experimental runs mentioned above were repeated three times.

After pyrolysis, the autoclave was washed thoroughly with toluene. Following the Industrial Standard of Chinese Petrochemical NB/SH/T 0509-2010, the collected pyrolysis product was separated into gas, coke, asphaltenes, and maltenes. The weight fractions of each component in the product were evaluated by

$$Y_i = \frac{m_i}{\sum m_i} \times 100\% \tag{1}$$

where m_i represents the weight of the component collected. The subscript i=As, M, C, and G represents asphaltenes, maltenes, coke, and gas. For the reaction concerning autocatalysis, the weight of the coke added into the feedstock was subtracted from that of the coke collected in the product.

The mass balance of experimental runs was determined by

$$\mathrm{MB} = \frac{\sum m_i}{m_{\mathrm{raw}}} \times 100\% \tag{2}$$

where m_{raw} is the weight of the loaded heavy oil. Normally, the values of MB varied between 92 and 96%.

Results and Discussion

Pyrolysis behavior under SCW and N_2 environments

The reaction kinetics of the pyrolysis of heavy oil in the presence of SCW were measured at a fixed water density of 0.25 g/cm^3 and three temperatures of 663, 683, and 703 K. During the reaction, the pressure varied between 23 and

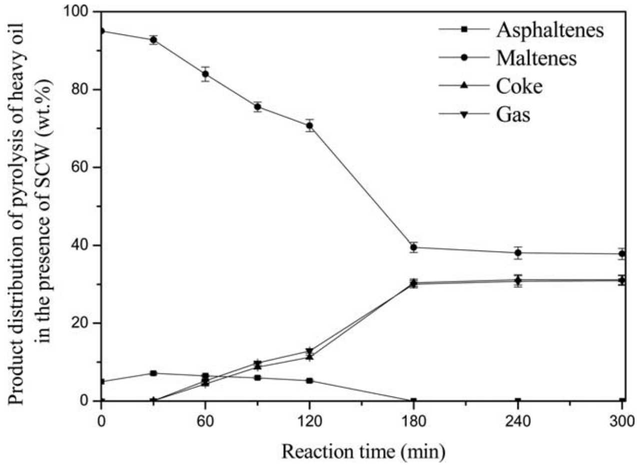

Figure 1. Product distribution of pyrolysis of heavy oil in the presence of SCW; reaction temperature of 663 K.

31 MPa. Typical product distributions at extended reaction times are illustrated in Figures 1 and 2.

Along with the extension of reaction time, the fraction of maltenes in the product decreases consistently and the fractions of coke and gas increase oppositely. The fraction of asphaltenes in the product varies differently with respect to the reaction temperature applied. At the temperature of 663 K, the value of Y_{As} increases from the initial value of 5.0 wt % to a maximum value of 7.1 wt % at the reaction time of 30 min, maintaining at that level for nearly 90 min. Then, it falls to zero within the following 60 min's reaction. At the temperature of 703 K, the value of Y_{As} decreases monotonically, approaching zero merely at the reaction time of 30 min. After pyrolysis, liquid products containing polycyclic aromatics could be obtained. Over the temperature range applied, the reactivity of these light oil fractions is much lower than that of the raw heavy oil. No more abrupt change in the product distribution can be observed once the value of Y_{C} reaches a value around 31.0 wt %. Provided that the pyrolysis is terminated at a limited reaction time, a pseudoequilibrium among maltenes, coke and gas is supposed to be established.

Although the fractions of maltenes, coke, and gas in the product all change monotonically during pyrolysis, their way of approaching equilibrium actually differs greatly at increasing temperatures. At the temperature of 663 K, the values of Y_{M}, Y_{C}, and Y_{G} vary smoothly at the start of the reaction. The variation becomes remarkable at the reaction time of 30 min but slows down again at the reaction time of 180 min. Consequently, the yields of these components all present a typical sigmoid pattern. At the temperature of 703 K, the value of Y_{M} decreases drastically along a concave downward curve and it is balanced mostly by the simultaneous increase in the values of Y_{C} and Y_{G} along convex upward curves.

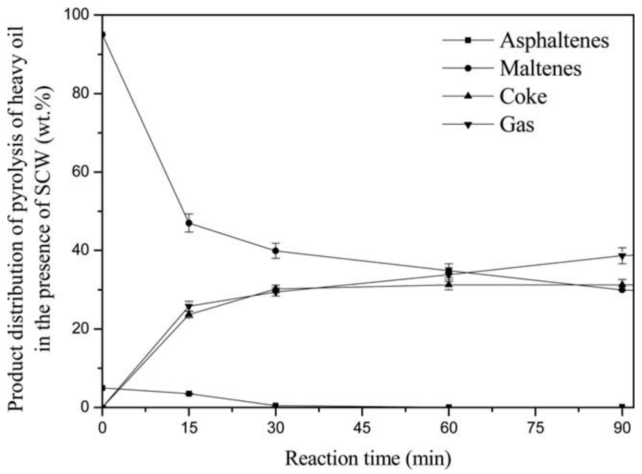

Figure 2. Product distribution of pyrolysis of heavy oil in the presence of SCW; reaction temperature of 703 K.

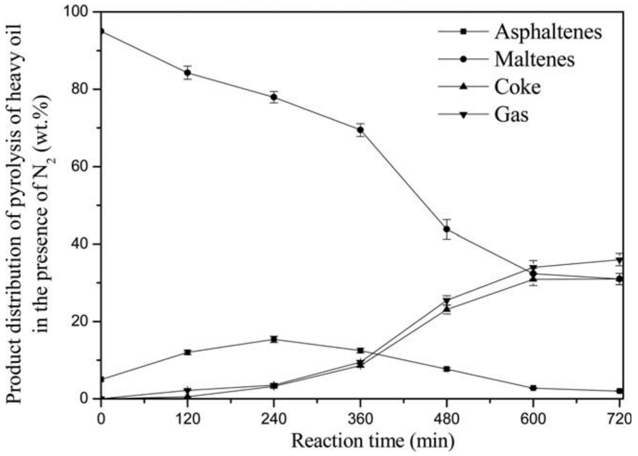

Figure 3. Product distribution of pyrolysis of heavy oil in the presence of N_2; reaction temperature of 663 K.

To have a full picture of pyrolysis, the reaction kinetics of the pyrolysis of heavy oil in the presence of N_2 were also measured at the same temperatures, during which the reaction pressure varied between 19 and 20 MPa. Typical product distributions at extended reaction times are illustrated in Figures 3 and 4. The time axes in Figures 3 and 4 range from 0 to 720 min, which are more than 2 times those in Figures 1 and 2.

The reaction behavior of the pyrolysis under N_2 environments is similar to that under SCW environments; still, there are some delicate differences between them. At three temperatures, the fractions of coke and gas in the product always vary along sigmoid curves. During the reaction, the fraction of asphaltenes in the product could be up to 16.0 wt %, which is

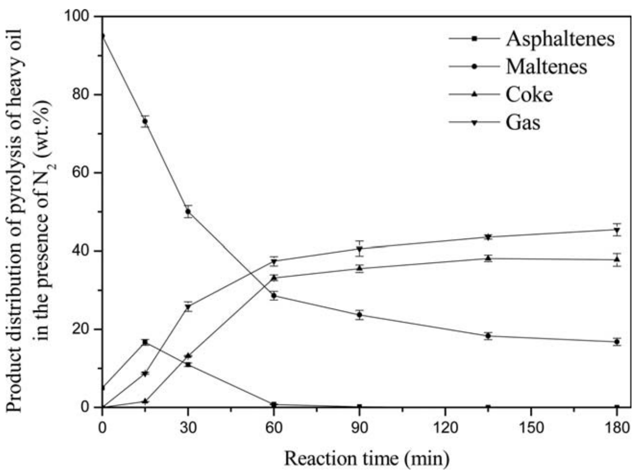

Figure 4. Product distribution of pyrolysis of heavy oil in the presence of N_2; reaction temperature of 703 K.

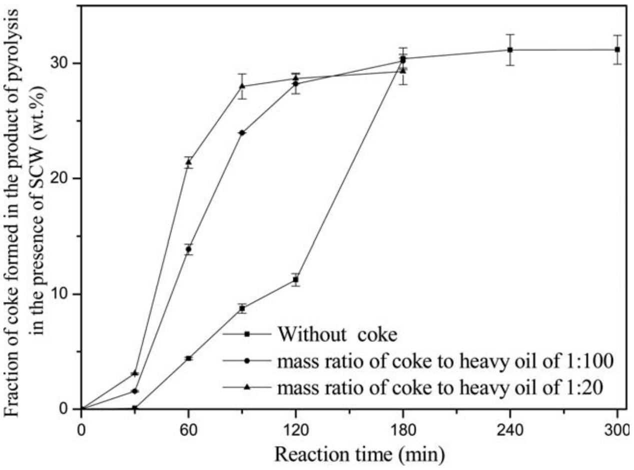

Figure 5. Rate of coke formation at varied coke additions as catalyst in pyrolysis of heavy oil in the presence of SCW; reaction temperature of 663 K.

much higher than the corresponding value observed under SCW environments.

Comparing the kinetic data presented in Figures 1–4, one may find that the pyrolysis of heavy oil under SCW environments is significantly accelerated. Take the pyrolysis at the temperature of 703 K as an example. Only after 15 min's reaction under SCW environments, the fraction of maltenes in the product has already decreased from its initial value of 95.0 to 47.0 wt %. Also, a high fraction of coke of 23.7 wt % could be observed. Under the same operating condition, the value of Y_M under N_2 environments remains at a high level of 73.1 wt %. Meanwhile, the formation of coke, whose fraction in the product is merely 1.5 wt %, can nearly be neglected.

Characteristic of autocatalysis of pyrolysis

No matter the pyrolysis of heavy oil is run under SCW or N_2 environments, the fractions of maltenes, coke, and gas in the products could vary along sigmoid curves, indicating the possible autocatalytic characteristic of pyrolysis. By this consideration, a small amount of coke was added into the feedstock.

According to the data presented in Figure 5, the formation of coke during the pyrolysis of heavy oil under SCW environments is accelerated by the introduction of coke in the feedstock. At the reaction temperature of 663 K, it takes about 180 min for the pyrolysis to approach pseudoequilibrium. The corresponding time is drastically reduced to 120 and 90 min when coke is added with the increasing mass ratios of coke to heavy oil from 1:100 to 1:20. Since coke is the ultimate product of the sequential condensation of maltenes and asphaltenes, the pyrolysis of heavy oil appears to be accelerated by the coke formed.

With a fixed coke addition at the mass ratio of coke to heavy oil of 1:100, the pyrolysis was further applied at increasing temperatures, with the results illustrated in Figure 6. For comparison, the data of the pyrolysis without the addition of coke are also included. At the temperature of 663 K the formation of coke during the pyrolysis with coke addition is much faster than that without coke addition, although they both vary along sigmoid curves. At the reaction time of 120 min, a pseudoequilibrium has almost been established for the pyrolysis with coke addition, while the pyrolysis without coke addition is still far away from pseudoequilibrium. When the reaction temperature is increased to 683 K, the yield of coke with coke addition varies along a convex upward curve rather than the original sigmoid curve. At that time, only a difference in the initial rate of coke formation could be identified. At the reaction temperature of 703 K, one can hardly tell the essential difference in the rate of coke formation between the pyrolysis with and without coke addition.

Similar phenomena can also be observed for the pyrolysis run under N_2 environments, but the acceleration to the pyrolysis resulted from coke addition in the feedstock is just less effective. Based on the data presented, the autocatalytic characteristic of the pyrolysis of heavy oil can be confirmed. In addition, such a characteristic is weakened with the increase in reaction temperature.

Development of lumped reaction kinetic models

The condensation of polycyclic aromatics and the dealkylation of substituents of polycyclic aromatics occur simultaneously during the pyrolysis of heavy oil.[35] Usually, the former has a dominant role on the product distribution observed. The decomposition of alkyl sulfides in SCW may partly contribute to the dealkylation.[16] However, its influence on the condensation of polycyclic aromatics is just marginal. Accordingly, only the reactions participated by hydrocarbons were considered here. Nevertheless, the structural isomer number of petroleum molecules grows exponentially with boiling point. As a compromise, lumping approaches are applied in the reaction kinetic models for the pyrolysis of heavy oil. It should be stressed that the reaction kinetic models based on the lumping approach actually are phenomenological models. Even the same model is used, the kinetic parameters vary substantially due to the difference in the properties of the raw heavy oil.

Although prominent progress has been made in structure oriented lumping, the lumping based on the traditional SARS separation has the advantages of the simple form and the clear definition of transformation.[36] According to the reaction network recommended by Yasar et al., a simplified network involving the condensation of maltenes to asphaltenes and the condensation of asphaltenes to coke and gas as illustrated in Figure 7 was adopted.[37] The traditional first-order lumped kinetic model, commonly used for the pyrolysis under N_2

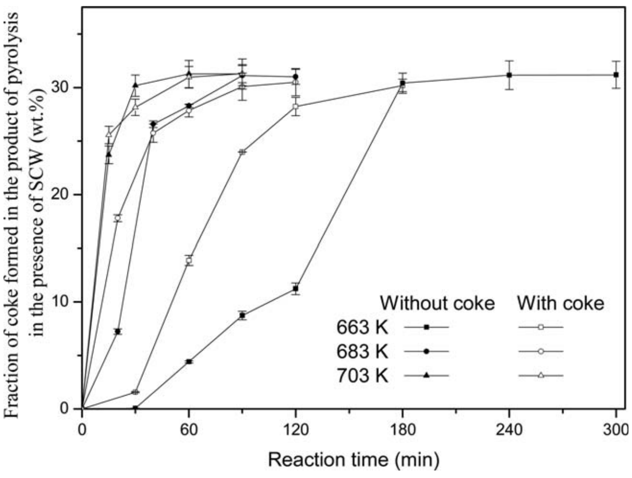

Figure 6. Rate of coke formation at varied reaction temperatures in pyrolysis of heavy oil without or with coke addition as catalyst; mass ratio of coke to heavy oil of 1:100.

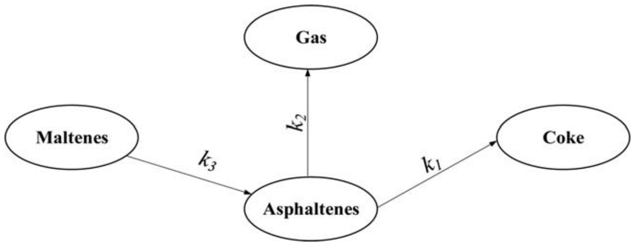

Figure 7. Four-lump reaction network for pyrolysis of heavy oil.

environments, then was modified. The development of the traditional and three modified models is sketched as follows.

Model I (First-Order Reaction Network). Many a research considered the transformation of lumped components involved in the pyrolysis of heavy oil as a pseudo first-order reaction, although there are huge differences in the molecular weight, chemical structure and physical properties between lumped components.[38–42] The traditional first-order kinetic model I is expressed by

$$-dC_{\mathrm{As}}/dt=(k_1+k_2)C_{\mathrm{As}}-k_3C_{\mathrm{M}} \tag{3}$$

$$-dC_{\mathrm{M}}/dt=k_3C_{\mathrm{M}} \tag{4}$$

$$-dC_{\mathrm{C}}/dt=-k_1C_{\mathrm{As}} \tag{5}$$

$$-dC_{\mathrm{G}}/dt=-k_2C_{\mathrm{As}} \tag{6}$$

where C_{As}, C_{M}, C_{C}, and C_{G} in units of kg/L are the weight concentrations of the lumped component in the reaction system.

Model II (Autocatalysis of Condensation). The experimental results have confirmed that the pyrolysis of heavy oil can be accelerated by the coke formed. Model II with the modification of autocatalysis is expressed by

$$-dC_{\mathrm{As}}/dt=(k_1+k_2)C_{\mathrm{As}}C_{\mathrm{C}}{}^{\alpha}-k_3C_{\mathrm{M}}C_{\mathrm{C}}{}^{\beta} \tag{7}$$

$$-dC_{\mathrm{M}}/dt=k_3C_{\mathrm{M}}C_{\mathrm{C}}{}^{\beta} \tag{8}$$

$$-dC_{\mathrm{C}}/dt=-k_1C_{\mathrm{As}}C_{\mathrm{C}}{}^{\alpha} \tag{9}$$

$$-dC_{\mathrm{G}}/dt=-k_2C_{\mathrm{As}}C_{\mathrm{C}}{}^{\alpha} \tag{10}$$

where parameters α and β are the reaction orders with respect to the weight concentration of coke in the reaction system.

Model III (Constraint of Pseudoequilibrium). Over the temperature range applied, a pseudoequilibrium among maltenes, coke and gas can be established within limited reaction time. The condensation of maltenes and asphaltenes is driven by the difference in the concentration with respect to their pseudoequilibrium values. The closer the reaction approaches equilibrium, the lower the driving force is. Model III with the consideration of pseudoequilibrium is expressed by

$$-dC_{\mathrm{As}}/dt=(k_1+k_2)(C_{\mathrm{As}}-C_{\mathrm{As.eq}})-k_3(C_{\mathrm{M}}-C_{\mathrm{M.eq}}) \tag{11}$$

$$-dC_{\mathrm{M}}/dt=k_3(C_{\mathrm{M}}-C_{\mathrm{M.eq}}) \tag{12}$$

$$-dC_{\mathrm{C}}/dt=-k_1(C_{\mathrm{As}}-C_{\mathrm{As.eq}}) \tag{13}$$

$$-dC_{\mathrm{G}}/dt=-k_2(C_{\mathrm{As}}-C_{\mathrm{As.eq}}) \tag{14}$$

where $C_{\mathrm{M.eq}}$ and $C_{\mathrm{As.eq}}$ in units of kg/L are the pseudoequilibrium weight concentrations of maltenes and asphaltenes in the reaction system.

Model IV (Autocatalysis of Condensation and Constraint of Pseudoequilibrium). It is assumed that the reaction kinetics of pyrolysis are influenced simultaneously by autocatalysis and pseudoequilibrium. Model IV with both modifications is expressed by

$$-dC_{\mathrm{As}}/dt=(k_1+k_2)(C_{\mathrm{As}}-C_{\mathrm{As.eq}})C_{\mathrm{C}}{}^{\alpha}-k_3(C_{\mathrm{M}}-C_{\mathrm{M.eq}})C_{\mathrm{C}}{}^{\beta} \tag{15}$$

$$-dC_{\mathrm{M}}/dt=k_3(C_{\mathrm{M}}-C_{\mathrm{M.eq}})C_{\mathrm{C}}{}^{\beta} \tag{16}$$

$$-dC_{\mathrm{C}}/dt=-k_1(C_{\mathrm{As}}-C_{\mathrm{As.eq}})C_{\mathrm{C}}{}^{\alpha} \tag{17}$$

$$-dC_{\mathrm{G}}/dt=-k_2(C_{\mathrm{As}}-C_{\mathrm{As.eq}})C_{\mathrm{C}}{}^{\alpha} \tag{18}$$

The parameters to be determined in Eqs. 3–18 are rate constants k_1, k_2, and k_3 as well as reaction orders α and β. Parameter identification relies on solving the nonlinear least-squares problem U by minimizing the weighted residual sum of squares (RSS) criterion.

$$\begin{cases} \mathrm{RSS}\left(\vec{k},\alpha,\beta\right)=\sum_{i=1}^{n}\sum_{j=1}^{m}w_j\left(\overline{C_{ij}}-C_{ij}\right)^2)/n \\ \vec{k}=\{k_1,k_2,k_3\}\geq 0;\ \ \alpha,\beta\geq 0 \end{cases} \tag{19}$$

where C_{ij} is the concentration of the j th lumped component from the i th experimental run in the kinetic data set $P=\{P_i,\ i=1,\ n;\ P_i\in\Re_n\}$, and the bar stands for the model predicted values. $w_j=\{5,1,1,1\}$ is the optimized weight of asphaltenes, maltenes, coke, and gas adopted in minimization.

With the software package of MATLAB R2012, the kinetic parameters were estimated by a multivariable nonlinear minimization combined with a Runge-Kutta integration algorithm. The adaptability of reaction kinetic models for the pyrolysis in both reaction media was evaluated according to the RSS analysis and the F-test at the 5% significance level.

Adaptability of lumped reaction kinetic models for pyrolysis

Initially the mixture of heavy oil and SCW exists with an oil/SCW two-phase structure. By the difference in polarity, maltenes and asphaltenes are distributed between the oil and SCW phases spontaneously. Ideally, the pyrolysis at that time can be divided into the condensation of maltenes in the SCW phase and the condensation of asphaltenes in the oil phase. The total fraction of coke and gas in the ultimate pyrolysis product can be up to about 70.0 wt %, which is much higher than the initial fraction of asphaltenes detained in the oil phase. Provided that maltenes are mostly dissolved into the SCW phase, there is a good chance that the sequential condensation of maltenes and asphaltenes transferred into the SCW phase plays a vital role on the pyrolysis under SCW environments. To this end, a high water density and a high water to oil ratio were adopted. Also, the rate of the dissolution of maltenes into the SCW phase was guaranteed by vigorous agitation. On the contrary, the pyrolysis under N_2 environments occurs either in the continuous oil phase under static condition or in the dispersed oil droplets under vigorous stirring. With the operating conditions applied in this work, the pyrolysis under SCW and N_2 environments therefore reflects approximately the characteristics of the reaction occurring in the SCW phase and in the oil phase. Based on models I to IV, the corresponding kinetic parameters of the pyrolysis of heavy oil in the SCW and oil phases were estimated, with the results listed in Tables 2–5. The results of RSS analysis and F-test are also attached in these tables.

Table 2. Kinetic Parameters of Pyrolysis of Heavy Oil in SCW Phase with Kinetic Models I and III

Model	Temperature (K)	k_1 (min^{-1})	k_2 (min^{-1})	k_3 (min^{-1})	RSS×10^3	F-test (5%)
I	663	2.70 E −02	2.72 E −02	3.50 E −03	1.00 E +01	Failed
	683	7.91 E −02	8.52 E −02	1.11 E −02	1.90 E +01	Failed
	703	3.36 E −01	3.80 E −01	2.12 E −02	1.70 E +01	Failed
III	663	2.44 E −02	2.48 E −02	7.90 E −03	1.02 E +01	Pass
	683	7.03 E −02	7.50 E −02	2.99 E −02	8.60 E +00	Pass
	703	2.83 E −01	3.32 E −01	6.25 E −02	6.40 E +00	Pass

Table 3. Kinetic Parameters of Pyrolysis of Heavy Oil in SCW Phase with Kinetic Models II and IV

Model	Temperature (K)	k_1 (kg L^{-1})$^{-\alpha}$min^{-1}	k_2 (kg L^{-1})$^{-\alpha}$min^{-1}	k_3 (kg L^{-1})$^{-\beta}$min^{-1}	α	β	RSS×10^3	F-test (5%)
II	663	5.09 E −01	5.11E −01	1.15E −02	5.73E −01	2.37 E −01	7.28 E +00	Pass
	683	4.22 E −01	4.53 E −01	1.11 E −02	4.01 E −01	0.00 E +00	1.65 E +01	Pass
	703	4.87 E −01	5.52 E −01	2.11 E −02	1.09 E −01	0.00 E +00	1.69 E +01	Pass
IV	663	8.51 E −01	8.67 E −01	3.10 E −01	6.45 E −01	6.80 E −01	4.75 E +00	pass
	683	1.09 E −01	1.16 E −01	3.00 E −02	1.16 E −01	0.00 E +00	8.06 E +00	Pass
	703	2.83 E −01	3.32 E −01	6.25 E −02	0.00E +00	0.00 E +00	6.40 E +00	Pass

Table 4. Kinetic Parameters of Pyrolysis of Heavy Oil in Oil Phase with Kinetic Model I

Model	Temperature (K)	k_1 (min^{-1})	k_2 (min^{-1})	k_3 (min^{-1})	RSS×10^3	F-test (5%)
I	663	4.40 E −03	4.90 E −03	1.50 E −03	1.45 E +01	Pass
	683	1.80 E −02	2.08 E −02	5.70 E −03	1.28 E +01	Pass
	703	5.29 E −02	6.28 E −02	1.94 E −02	1.37 E +01	Pass

Reaction in the SCW phase

Model I. At the temperatures ranging from 663 to 703 K, the RSS values given by model I always maintain at a high level. What is worse, the model predicted product distributions all fail to pass the following F-test. For ordinary differential Eqs. 3–6, actually there exists an analytical solution as follows.

$$C_{\mathrm{As}}=C_{\mathrm{As.0}}\exp(-(k_1+k_2)t)+\frac{k_3C_{\mathrm{M.0}}[\exp(-k_3t)-\exp(-(k_1+k_2)t)]}{k_1+k_2-k_3} \tag{20}$$

$$C_{\mathrm{M}}=C_{\mathrm{M.0}}\exp(-k_3t) \tag{21}$$

$$C_{\mathrm{C}}=\frac{k_1}{k_1+k_2}C_{\mathrm{T}}-\frac{\left[k_1C_{\mathrm{As.0}}-\frac{k_1k_3}{k_1+k_2}C_{\mathrm{T}}\right]\exp(-(k_1+k_2)t)-k_1C_{\mathrm{M.0}}\exp(-k_3t)}{k_1+k_2-k_3} \tag{22}$$

$$C_{\mathrm{G}}=\frac{k_2}{k_1+k_2}C_{\mathrm{T}}-\frac{\left[k_1C_{\mathrm{As.0}}-\frac{k_2k_3}{k_1+k_2}C_{\mathrm{T}}\right]\exp(-(k_1+k_2)t)-k_1C_{\mathrm{M.0}}\exp(-k_3t)}{k_1+k_2-k_3} \tag{23}$$

where $C_{\mathrm{As.0}}$ and $C_{\mathrm{M.0}}$ in units of kg/L are the initial weight concentrations of asphaltenes and maltenes in the reaction system. C_{T}, the sum of $C_{\mathrm{As.0}}$ and $C_{\mathrm{M.0}}$, is the initial weight concentration of the raw heavy oil loaded.

Coke and gas are produced synchronously during pyrolysis. The values of k_1 and k_2 usually are close to each other, larger than that of k_3 by nearly one order of magnitude. Besides, C_{T} equals approximately to $C_{\mathrm{M.0}}$ since the value of $C_{\mathrm{As.0}}$ is only 5.0 wt %. By these considerations, Eqs. 22 and 23 can be simplified and take the form of

$$C_{\mathrm{c}}\approx C_{\mathrm{G}}\approx\frac{1}{2}C_{\mathrm{T}}[1-\exp(-k_3t)] \tag{24}$$

Within the framework of the first-order reaction network, the variation of the yields of maltenes, coke, and gas can only follow exponential functions, which is out of accord with the sigmoid pattern appearing at lower reaction temperatures. At the temperature of 663 K, the predicted values of Y_{C} and Y_{G} are inevitably higher than measured values at the early reaction stage but lower than measured values at the middle and later reaction stages. Even the yields of these lumped components do vary in accordance with exponential functions as expected at the temperature of 703 K, the drastic changes of Y_{M}, Y_{C}, and Y_{G} at the initial reaction stage as well as the smooth variation in the following process of approaching pseudoequilibrium deviate widely from the model predicted product distribution.

Models II and III. In view of the limitation of the first-order reaction network, model I was modified with autocatalysis

Table 5. Kinetic Parameters of Pyrolysis of Heavy Oil in Oil Phase with Kinetic Model IV

Model	Temperature (K)	k_1 (kg L^{-1})$^{-\alpha}$min^{-1}	k_2 (kg L^{-1})$^{-\alpha}$min^{-1}	k_3 (kg L^{-1})$^{-\beta}$min^{-1}	α	β	RSS×10^3	F-test (5%)
IV	663	9.85 E −02	1.11 E −01	1.95 E −02	6.42 E −01	3.64 E −01	6.89 E +00	Pass
	683	2.31 E −01	2.72 E −01	6.95 E −02	5.70 E −01	4.04 E −01	4.81 E +00	Pass
	703	3.74 E −01	4.47 E −01	5.93 E −02	4.60 E −01	1.55 E −01	4.42 E +00	Pass

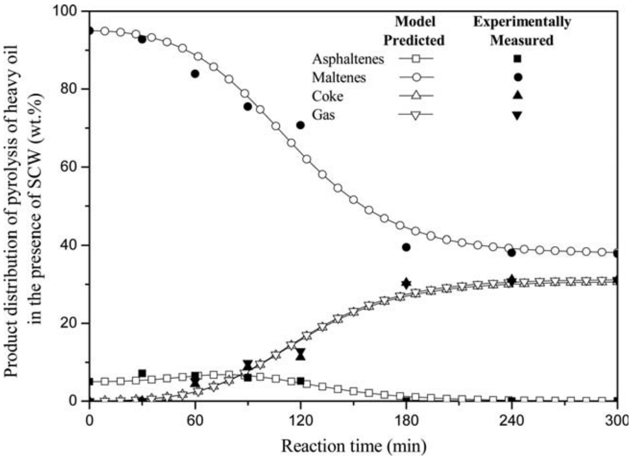

Figure 8. Model predicted vs. experimentally measured product distributions of pyrolysis in the presence of SCW; reaction temperature of 663 K; model IV.

and pseudoequilibrium, respectively. The fitting accuracy of models II and III to the product distribution measured depends strongly on the reaction temperature applied.

At the temperature of 663 K, the yields of maltenes, coke, and gas vary along sigmoid curves at the early and middle reaction stages, showing no evident variation approaching pseudoequilibrium. It can be deduced that the pyrolysis is governed successively by the autocatalysis of condensation and by the constraint of pseudoequilibrium. According to the data listed in Tables 2 and 3, the product distributions predicted by models II and III with a sole modification all pass the F-test. However, the RSS values given by these two models actually are at the same level with that given by model I.

The initiation of the pyrolysis network through the C—C cleavage of alkyl substitutes of polycyclic aromatics, a process driven by entropy change, has an extremely high reaction barrier. Of all operating parameters, the reaction temperature thus has the most prominent influence on the reaction kinetics of pyrolysis.[38,43,44] As the data presented in Figures 1 and 2 suggest, the pyrolysis in the SCW phase is significantly accelerated with the increase in reaction temperature. At the temperature of 703 K, the yields of maltenes, coke, and gas all vary along concave downward or convex upward curves rather than the sigmoid curves at the lower temperature of 663 K, suggesting the disappearance of the characteristic of autocatalysis. Such a tendency is in accordance with the data presented in Figure 6 in which the promotion to the pyrolysis with coke addition in the feedstock is weakened at increasing temperatures.

It is not surprising that at higher temperatures the fitting accuracy of model II with the sole modification of autocatalysis to pyrolysis remains poor. Even though, the reduced influence of autocatalysis on pyrolysis can be partly reflected by the estimated parameters α and β. At the temperatures of 683 K and higher, the value of β becomes zero. In the meantime, the value of α decreases from 0.57 to 0.11 along with the increase in reaction temperature from 663 to 703 K. By contrast, model III with the sole modification of pseudoequilibrium is capable of predicting the product distributions at the temperature of 683 and 703 K precisely since the reaction at that time is driven primarily by the difference with respect to pseudoequilibrium.

Model IV. With the combination of both modifications, the capability of model IV to describe the pyrolysis of heavy oil in the SCW phase is improved on the whole. On the one hand, the values of RSS are always controlled within a reasonable range. On the other hand, the model predicted product distributions all pass the F-test. A comparison between model predicted and experimentally measured product distributions at the temperature of 663 K is illustrated in Figure 8.

At the temperature of 663 K, the parameters α and β of model IV are 0.65 and 0.68, confirming the autocatalytic characteristic of condensation. Essentially, the condensation of maltenes is the two-dimensional extension of aromatic segments. The reaction barrier of the growth of coke-inducing components, mostly lower alkenes, on aromatic segments decreases with the increase in the aromaticity of condensed segments.[45,46] As for the condensation of asphaltenes, it is the subsequent three-dimensional stacking of aromatic segments. The coke formed during pyrolysis or the coke added in the feedstock can be templates for the stacking of aromatic segments. By the reaction mechanism involved, the condensation of maltenes and the condensation of asphaltenes both share the inherent characteristic of autocatalysis. It is interesting that the condensation of maltenes can benefit directly from the formation of coke.

At increasing reaction temperatures, the reaction kinetics of pyrolysis depend more on the promotion from the Arrhenius effect rather than on autocatalysis. As a result, the estimated parameters α and β of model IV decrease simultaneously. At the temperature of 683 K, the value of α is 0.12 and that of β reduces to zero. After a further increase in reaction temperature to 703 K, both parameters become zero. With the only characteristic of the constraint of pseudoequilibrium, model IV transforms into model III and the rate constants estimated by these two models become identical.

Reaction in the oil phase

Models I and IV. Despite of the change of reaction temperature, the product distribution of the pyrolysis in the oil phase always presents a similar variation tendency. According to the data listed in Table 4, the product distributions predicted by model I can pass the F-test. However, the corresponding RSS values maintain at a high level, a similar situation for the pyrolysis in the SCW phase.

With the modifications of autocatalysis and pseudoequilibrium, model IV is capable of describing the pyrolysis of heavy oil in the oil phase with satisfied accuracy. Based on the data listed in Table 5, the RSS value given by model IV at any reaction temperature is significantly lower than that given by model I by about 50 to 70%. Besides, the product distributions predicted all pass the following F-test. Typical results of the comparisons between model predicted and experimentally measured product distributions are illustrated in Figures 9 and 10.

At three temperatures, the estimated parameters α and β of model IV keep nonzero, which means the influence of autocatalysis should be considered. Similar to the reaction in the SCW phase, the estimated value of α is consistently higher than that of β, suggesting that the condensation of asphaltenes relies more on coke formation than the condensation of maltenes does. At increasing reaction temperatures, these two parameters both present a monotonically decreasing tendency. It is certain that the condensation of maltenes and the condensation of asphaltenes in the oil phase will disengage from the

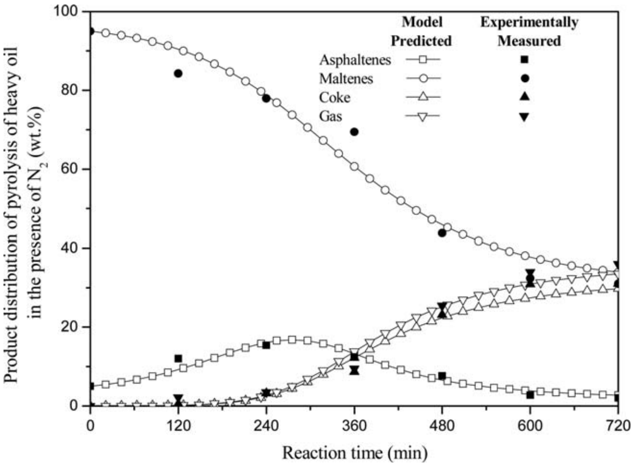

Figure 9. Model predicted vs. experimentally measured product distributions of pyrolysis in the presence of N_2; reaction temperature of 663 K; model IV.

influence of autocatalysis one after the other with a further increase in reaction temperature.

Effect of reaction media on reaction kinetics of pyrolysis

The pyrolysis of heavy oil in the presence of SCW may occur as an oil/water two-phase structure or as a single-phase. To make sure that maltenes were transferred into the SCW phase as much as possible, experiments were performed at a density of 0.25 g/cm^3 as this density has been shown to promote single-phase conditions in bitumen-SCW mixtures at temperatures similar to those used in this work.[29] With the further aid of a high water to oil ratio and vigorous agitation, the pyrolysis in the SCW phase could play a dominant role on the reaction behavior of the pyrolysis under SCW environments.

The pyrolysis of heavy oil is accomplished by condensation and dealkylation, involving a large number of bimolecular reactions, such as the H-abstraction from alkyl substitutes of polycyclic aromatics and the addition of alkenes to carbon radicals on polycyclic aromatics. These bimolecular reactions with a reaction barrier ranging from 30 to 60 kJ/mol are essential to the propagation of the pyrolysis network.[45–49] Reaction barriers of organic reactions usually varies from 40 to 400 kJ/mol. A lower reaction barrier indicates that the reaction kinetics of those elementary radical reactions involved in pyrolysis could be retarded by the presence of solvent molecules even when the reaction is run in the presence of a SCW phase.

For a fast reaction occurring in a solvent, the diffusion-limited rate constant k_d is directly proportional to the diffusivity of the solute.[50] Dabiri et al. recommended that the diffusion coefficient of a solute in SCW can be evaluated by the Tracer Liu–Silva–Macedo equation.[51–53] According to the measurement of molecular diffusivities using nuclear magnetic resonance, Kutney found that the diffusion coefficient of hydrocarbon species in dense SCW can be as high as 10^{-3} cm^2 s^{-1}.[54] Unfortunately, at high temperatures the corresponding data in heavy oil can hardly be found in the literature. Still, it is possible to evaluate approximately the influence of diffusivity on k_d since the diffusion coefficient of a solute in a solvent is inversely proportional to the viscosity of the solvent. Based on the temperature-viscosity correlation suggested by Alomair et al., the dynamic viscosity of heavy oil at the temperatures from 663 to 703 K varies around 1.0×10^{-3} Pa s.[55] During pyrolysis, the viscosity of the oil phase may decrease slightly because of the production of light oil fractions. By the IAPWS-95 formulation, the viscosity of water over the same temperature range varies merely from 3.3×10^{-5} to 3.7×10^{-5} Pa s. Provided that the bimolecular radical reaction occurring in the oil and SCW phases is both limited by diffusion, the value of k_d in the SCW phase therefore is supposed to be higher than that in the oil phase by 1 or 2 orders of magnitude.

The viscosity-based estimation of diffusion limitations is strictly an order of magnitude estimate and several additional factors need to be considered. In the near-critical and supercritical region of a solvent, dynamic solvent clusters surrounding solutes can be formed due to the interaction between the solute and the solvent.[56–58] The temperature range where significant clustering occurs in SCW is quite limited ($T_r < 1.05$) in contrast to the temperature dependence of the solvation in supercritical CF_3H and CO_2.[59] In terms of the scale of the cluster, the formation of solvent clusters can suppress the diffusion of solutes in the solvent to varying degrees.[60] Besides, the substantial dissolution of solutes into the SCW phase might result in a decrease in the diffusivity of the solute in SCW.[61] Despite these mitigating factors, the experimental data illustrated in Figures 1–4 are consistent with the conclusion that more rapid diffusion rates in the SCW phase accelerate pyrolysis reaction rates.

Benefited from the improved diffusion, the pyrolysis in the SCW phase is determined simultaneously by the diffusivity of hydrocarbon species and by the intrinsic reaction kinetics of the reactions involved. Accordingly, the pyrolysis occurring in the SCW phase responses more sensitively to the promotion from the Arrhenius effect than that in the oil phase does. At increasing temperatures, both the condensation of maltenes and the condensation of asphaltenes in the SCW phase may readily disengage from the dependence on autocatalysis. Within a narrow temperature range, the applicable kinetic model for the pyrolysis in the SCW phase transforms rapidly from model IV to model III with the sole modification of the constraint of pseudoequilibrium. By contrast, the pyrolysis in the oil phase is retarded by poor diffusion. Even at the temperature of 703 K, the reliance on autocatalysis is still responsible partly for the pyrolysis behavior under N_2 environments.

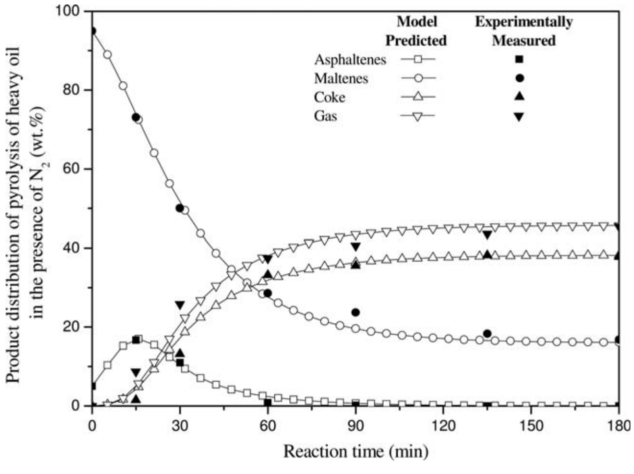

Figure 10. Model predicted vs. experimentally measured product distributions of pyrolysis in the presence of N_2; reaction temperature of 703 K; model IV.

Conclusions

By introducing SCW into the pyrolysis of heavy oil, the condensation of maltenes and asphaltenes can be partly or completely transferred from the oil phase into the SCW phase. The condensation occurring in the SCW phase was observed to be much faster than that in the oil phase. No matter the pyrolysis occurs in the oil or SCW phase, at lower temperatures the characteristics of the autocatalysis of condensation and the constraint of pseudoequilibrium appear successively. At that time, the pyrolysis in both phases can be accurately described by the first-order lumped reaction kinetic model modified with both characteristics. With the increase in reaction temperature, the characteristic of autocatalysis disappears. Accordingly, the pyrolysis can be described by the first-order lumped kinetic model modified with the sole constraint of pseudoequilibrium. Due to the significantly improved diffusion, the pyrolysis in the SCW phase is more sensitive to the variation of reaction temperature than the pyrolysis in the oil phase is. At increasing reaction temperatures, the pyrolysis in the SCW phase disengages rapidly from the influence of autocatalysis.

Acknowledgments

This work was supported by the CNPC Innovation Foundation (2011D-5006-0406), the Open Project of State Key Laboratory of Chemical Engineering (SKL-ChE-13C02), and the National Natural Science Foundation of China (Grant No. 21376075).

Notation

$C_{\mathrm{As.eq}}$ = pseudoequilibrium weight concentration of asphaltenes in the reaction system, kg L^{-1}
$C_{\mathrm{As.0}}$ = initial weight concentration of asphaltenes in the reaction system, kg L^{-1}
C_i = weight concentration of lumped components in the reaction system, kg L^{-1}
$C_{\mathrm{M.eq}}$ = pseudoequilibrium weight concentration of maltenes in the reaction system, kg L^{-1}
$C_{\mathrm{M.0}}$ = initial weight concentration of maltenes in the reaction system, kg L^{-1}
C_{T} = initial weight concentration of the raw heavy oil in the reaction system, kg L^{-1}
k_i = rate constant of the transformation between lumped components, min^{-1}, $(\mathrm{kg\ L}^{-1})^{-\alpha}\mathrm{min}^{-1}$ or $(\mathrm{kg\ L}^{-1})^{-\beta}\mathrm{min}^{-1}$
k_{d} = diffusion-limited rate constant, L mol^{-1} s^{-1}
m_i = weight of the lumped components collected, kg
m_{raw} = weight of the raw heavy oil loaded, kg
t = reaction time, min
Y_i = weight fraction of lumped components in the pyrolysis product

Greek letters

α = reaction order with respect to the concentration of coke in the condensation of asphaltenes
β = reaction order with respect to the concentration of coke in the condensation of maltenes

Literature Cited

1. Bolonkin A, Friedlander J, Neumann S. Innovative unconventional oil extraction technologies. *Fuel Process Technol*. 2014;124:228–242.
2. Javad S, Oskouei P, Maini B, Moore RG, Mehta SA. Experimental evaluation of SAGD/ISC hybrid recovery method. *J Can Pet Technol*. 2013;52(3):204–218.
3. Guo HF, Peng SY, Lin JD, Chang J, Lei S, Fan TB, Liu YY. Retorting oil shale by a self-heating route. *Energy Fuels*. 2013;27(5):2445–2451.
4. Rana MS, Samano V, Ancheyta J, Diaz JAI. A review of recent advances on process technologies for upgrading of heavy oils and residua. *Fuel*. 2007;86(9):1216–1231.
5. Sawarkar AN, Pandit AB, Samant SD, Joshi JB. Petroleum residue upgrading via delayed coking: a review. *Can J Chem Eng*. 2007; 85(1):1–24.
6. Matsui Y, Katayama R, Tamura Y, Teratani S, Ota M, Sato Y, Inomata H. Measurements of water-heavy oil phase equilibrium for supercritical water upgrading process. *J Jpn Pet Inst*. 2014;57(3): 118–124.
7. Morimoto M, Sugimoto Y, Sato S, Takanohashi T. Bitumen cracking in supercritical water upflow. *Energy Fuels*. 2014;28(2):858–861.
8. Sato T. Upgrading of heavy oil by hydrogenation through partial oxidation and water-gas shift reaction in supercritical water. *J Jpn Pet Inst*. 2014;57(1):1–10.
9. Morimoto M, Sugimoto Y, Sato S, Takanohashi T. Solvent effect of water on supercritical water treatment of heavy oil. *J Jpn Pet Inst*. 2014;57(1):11–17.
10. Furimsky E. Hydroprocessing in aqueous phase. *Ind Eng Chem Res*. 2013;52(50):17695–17713.
11. Sato T, Adschiri T, Arai K, Rempel GL, Ng FTT. Upgrading of asphalt with and without partial oxidation in supercritical water. *Fuel*. 2003;82(10):1231–1239.
12. Arai K, Adschiri T, Watanabe M. Hydrogenation of hydrocarbons through partial oxidation in supercritical water. *Ind Eng Chem Res*. 2000;39(12):4697–4701.
13. Morimoto M, Sugimoto Y, Saotome Y, Sato S, Takanohashi T. Effect of supercritical water on upgrading reaction of oil sand bitumen. *J Supercrit Fluids*. 2010;55(1):223–231.
14. Caniaz RO, Erkey C. Process intensification for heavy oil upgrading using supercritical water. *Chem Eng Res Des*. 2014;92(10):1845–1863.
15. Timko MT, Ghoniem, AF, Green, WH. Upgrading and desulfurization of heavy oils by supercritical water. *J Supercrit Fluids*. 2015; 96:114–123.
16. Kida Y, Class CA, Concepcion AJ, Timko MT, Green WH. Combining experiment and theory to elucidate the role of supercritical water in sulfide decomposition. *Phys Chem Chem Phys*. 2014;16(20):9220–9228.
17. Patwardhan PR, Timko MT, Class CA, Bonomi RE, Kida Y, Hernandez HH, Tester JW, Green WH. Supercritical water desulfurization of organic sulfides is consistent with free-radical kinetics. *Energy Fuels*. 2013;27(10):6108–6117.
18. Pinto LDS, dos Santos LMF, Al-Duri B, Santos RCD. Supercritical water oxidation of quinoline in a continuous plug flow reactor - part 1: effect of key operating parameters. *J Chem Technol Biotechnol*. 2006;81(6):912–918.
19. Adschiri T, Shibata R, Sato T, Watanabe M, Arai K. Catalytic hydrodesulfurization of dibenzothiophene through partial oxidation and a water-gas shift reaction in supercritical water. *Ind Eng Chem Res*. 1998;37(7):2634–2638.
20. Yuan PQ, Cheng ZM, Zhang XY, Yuan WK. Catalytic denitrogenation of hydrocarbons through partial oxidation in supercritical water. *Fuel*. 2006;85(3):367–373.
21. Yuan PQ, Cheng ZM, Jiang WL, Zhang R, Yuan WK. Catalytic desulfurization of residual oil through partial oxidation in supercritical water. *J Supercrit Fluids*. 2005;35(1):70–75.
22. Cheng ZM, Ding Y, Zhao LQ, Yuan PQ, Yuan WK. Effects of supercritical water in vacuum residue upgrading. *Energy Fuels*. 2009;23(6):3178–3183.
23. Moriya T, Enomoto H. Role of water in conversion of polyethylene to oils through supercritical water cracking. *Kagaku Kogaku Ronbunshu*. 1999;25(6):940–946.
24. Moriya T, Enomoto H. Conversion of polyethylene to oil using supercritical water and donation of hydrogen in supercritical water. *Kobunshi Ronbunshu*. 2001;58(12):661–673.
25. Zhu CC, Ren C, Tan XC, Chen G, Yuan PQ, Cheng ZM, Yuan WK. Initiated pyrolysis of heavy oil in the presence of near-critical water. *Fuel Process Technol*. 2013;111:111–117.
26. Han LN, Zhang R, Bi JC. Experimental investigation of high-temperature coal tar upgrading in supercritical water. *Fuel Process Technol*. 2009;90(2):292–300.
27. Zhao LQ, Cheng ZM, Ding Y, Yuan PQ, Lu SX, Yuan WK. Experimental study on vacuum residuum upgrading through pyrolysis in supercritical water. *Energy Fuels*. 2006;20(5):2067–2071.
28. Watanabe M, Kato SN, Ishizeki S, Inomata H, Smith RL Jr. Heavy oil upgrading in the presence of high density water: basic study. *J Supercrit Fluids*. 2010;53(1–3):48–52.
29. Amani MJ, Gray MR, Shaw JM. Phase behavior of Athabasca bitumen + water mixtures at high temperature and pressure. *J Supercrit Fluids*. 2013;77:142–152.

30. Amani MJ, Gray MR, Shaw JM. The phase behavior of Athabasca bitumen + toluene + water ternary mixtures. *Fluid Phase Equilib*. 2014;370:75–84.
31. Amani MJ, Gray MR, Shaw JM. Volume of mixing and solubility of water in Athabasca bitumen at high temperature and pressure. *Fluid Phase Equilib*. 2013;358:203–211.
32. Brunner E, Thies MC, Schneider GM. Fluid mixtures at high pressures: phase behavior and critical phenomena for binary mixtures of water with aromatic hydrocarbons. *J Supercrit Fluids*. 2006;39(2):160–173.
33. Vilcaez J, Watanabe M. Watanabe N, Kishita A, Adschiri T. Hydrothermal extractive upgrading of bitumen without coke formation. *Fuel*. 2012;102:379–385.
34. Tan XC, Liu QK, Zhu DQ, Yuan PQ, Cheng ZM, Yuan WK. Pyrolysis of heavy oil in the presence of supercritical water: the reaction kinetics in different phases. *AIChE J*. 2015;61(3):857–866.
35. Kozhevnikov IV, Nuzhdin AL, Martyanov ON. Transformation of petroleum asphaltenes in supercritical water. *J Supercrit Fluids*. 2010;55(1):217–222.
36. Zhang LZ, Hou Z, Horton SR, Klein MT, Shi Q, Zhao SQ, Xu CM. Molecular representation of petroleum vacuum resid. *Energy Fuels*. 2014;28(3):1736–1749.
37. Yasar M, Trauth DM, Klein MT. Asphaltene and resid pyrolysis. 2. The effect of reaction environment on pathways and selectivities. *Energy Fuels*. 2001;15(3):504–509.
38. Singh J, Kumar MM, Saxena AK, Kumar S. Reaction pathways and product yields in mild thermal cracking of vacuum residues: a multi-lump kinetic model. *Chem Eng J*. 2005;108(3): 239–248.
39. Carlo SD, Janis B. Composition and visbreakability of petroleum residues. *Chem Eng Sci*. 1992;47(9–11):2695–2700.
40. Kataria KL, Kulkarni RP, Pandit AB, Joshi JB, Kumar M. Kinetic studies of low severity visbreaking. *Ind Eng Chem Res*. 2004;43(6): 1373–1387.
41. Ancheyta J, Sánchez S, Rodríguez MA. Kinetic modeling of hydrocracking of heavy oil fractions: a review. *Catal Today*. 2005;109(1–4):76–92.
42. Meng XH, Xu CM, Gao JS, Li L. Seven-lump kinetic model for catalytic pyrolysis of heavy oil. *Catal Commun*. 2007;8(8):1197–1201.
43. Geng AS, Liao ZW. Kinetic studies of asphaltene pyrolyses and their geochemical applications. *Appl Geochem*. 2002;17(12):1529–1541.
44. Liu Y, Bai F, Zhu CC, Yuan PQ, Cheng ZM, Yuan WK. Upgrading of residual oil in sub- and supercritical water: an experimental study. *Fuel Process Technol*. 2013;106:281–288.
45. Sabbe MK, Vandeputte AG, Reyniers MF, Speybroeck VV, Waroquier M, Marin GB. Ab initio thermochemistry and kinetics for carbon-centered radical addition and β-scission reactions. *J Phys Chem A*. 2007;111(34):8416–8428.
46. Speybroeck VV, Hemelsoet K, Waroquier M, Marine GB. Reactivity and aromaticity of polyaromatics in radical cyclization reactions. *Int J Quantum Chem*. 2004;96(6):568–576.
47. Hunter KC, East ALL. Properties of C-C bonds in n-alkanes: Relevance to cracking mechanisms. *J Phys Chem A*. 2002;106(7):1346–1356.
48. Xiao YT, Longo JM, Hieshima GB, Hill RJ. Understanding the kinetics and mechanisms of hydrocarbon thermal cracking: an ab initio approach. *Ind Eng Chem Res*. 1997;36(10):4033–4040.
49. Speybroeck VV, Neck DV, Waroquier MS, Saeys WM, Marin GB. Ab initio study of radical addition reactions: addition of a primary ethylbenzene radical to ethene (I). *J Phys Chem A*. 2000;104(46): 10939–10950.
50. Steinfeld JI, Francisco JS, Hase WL. *Chemical Kinetics and Dynamics*, 2nd ed. New Jersey: Prentice-Hall Inc., 1998:124–133.
51. Liu H, Silva CM, Macedo EA. Unified approach to the self-diffusion coefficients of dense fluids over wide ranges of temperature and pressure-hard-sphere, square-well, Lennard-Jones and real substances. *Chem Eng Sci*. 1998;53(13):2403–2422.
52. Dabiri S, Wu G, Timko MT, Ghoniem AF. Mixing of single-component hydrocarbon droplets and water at supercritical or near-critical conditions. *J Supercrit Fluids*. 2012;67:29–40.
53. Wu G, Dabiri S, Timko MT, Ghoniem AF. Fractionation of multi-component hydrocarbon droplets in water at supercritical, or near-critical conditions. *J Supercrit Fluids*. 2012;72:150–160.
54. Kutney MC. Thermodynamic and transport property modeling in supercritical water. Ph.D. Dissertation, Chemical Engineering, Massachusetts Institute of Technology, 2005. Available at: http://dspace.mit.edu/handle/1721.1/32335
55. Alomair O, Elsharkawy A, Alkandari H. A viscosity prediction model for Kuwaiti heavy crude oils at elevated temperatures. *J Pet Sci Technol*. 2014;120:102–110.
56. Duan JS, Shim Y, Kim HJ, Solvation in supercritical water. *J Chem Phys*. 2006;124(20):204504–204516.
57. Fujisawa T, Terazima M, Kimura Y, Maroncelli M. Resonance Raman study of the solvation of p-nitroaniline in supercritical water. *Chem Phys Lett*. 2006;430(4–6):303–308.
58. Cummings PT, Cochran HD, Simonson JM, Mesmer RE, Karaborni S. Simulation of supercritical water and of supercritical aqueous solutions. *J Chem Phys*. 1991;94(8):5606–5621.
59. Oka H, Kajimoto O. UV absorption solvatochromic shift of 4-nitroaniline in supercritical water. *Phys Chem Chem Phys*. 2003;5: 2535–2540.
60. Yuan PQ, Zhu CC, Liu Y, Bai F, Cheng ZM, Yuan WK. Solvation of hydrocarbon radicals in sub-CW and SCW: an ab initio MD study. *J Supercrit Fluids*. 2011;58(1):93–98.
61. Brunner G. *Hydrothermal and Supercritical Water Processes*. Burlington: Elsevier Science, 2014:98–110.

Manuscript received Dec. 10, 2014, and revision received July 30, 2015.